Science of the Total Environment 915 (2024) 169966

Contents lists available at ScienceDirect

Science of the Total Environment

journal homepage: www.elsevier.com/locate/scitotenv

Research Paper

The transition between coastal and offshore areas in the North Sea unraveled by suspended particle composition

Xavier Desmit [a,*], Markus Schartau [b], Rolf Riethmüller [c], Nathan Terseleer [a], Dimitry Van der Zande [a], Michael Fettweis [a]

[a] OD Natural Environment, Royal Belgian Institute of Natural Sciences, Vautier Street 29, 1000 Brussels, Belgium
[b] GEOMAR Helmholtz Centre for Ocean Research Kiel, Wischhofstr. 1-3 D-24148 Kiel, Germany
[c] Institute of Coastal Ocean Dynamics, Helmholtz-Zentrum Hereon, Max-Planck-Str. 1, 21502 Geesthacht, Germany

HIGHLIGHTS

- SPM concentration and organic fractions are analyzed in coastal-offshore gradients
- Diagnostic model of SPM allows separating fresh, labile from less reactive PON
- Analysis of PON fractions reveals a characteristic area, the transition zone
- There, particle settling is enhanced, fostering their transport back to the coast, which controls the fate of organic matter
- The transition zone is generally confined to water depths below 20 m

GRAPHICAL ABSTRACT

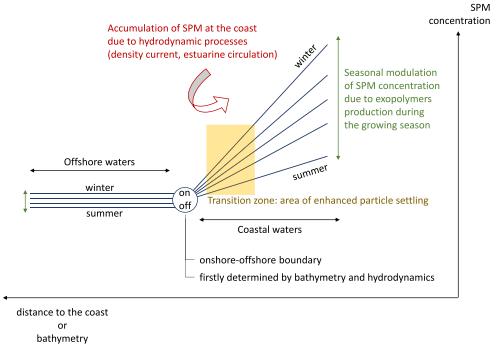

ARTICLE INFO

Editor: Daniel Alessi

Keywords:
Suspended particulate matter (SPM)
Particulate organic nitrogen (PON)
Particle dynamics
Particle composition
Coastal-offshore gradient
North Sea

ABSTRACT

Identifying the mechanisms that contribute to the variability of suspended particulate matter concentrations in coastal areas is important but difficult, especially due to the complexity of physical and biogeochemical interactions involved. Our study addresses this complexity and investigates changes in the horizontal spread and composition of particles, focusing on cross-coastal gradients in the southern North Sea and the English Channel. A semi-empirical model is applied on in situ data of SPM and its organic fraction to resolve the relationship between organic and inorganic suspended particles. The derived equations are applied onto remote sensing products of SPM concentration, which provide monthly synoptic maps of particulate organic matter concentrations (here, particulate organic nitrogen) at the surface together with their labile and less reactive fractions. Comparing these fractions of particulate organic matter reveals their characteristic features along the coastal-offshore gradient, with an area of increased settling rate for particles generally observed between 5 and 30 km from the coast. We identify this area as the transition zone between coastal and offshore waters with respect to particle dynamics. Presumably, in that area, the turbulence range and particle composition favor particle settling, while hydrodynamic processes tend to transport particles of the seabed back towards the coast. Bathymetry plays an important role in controlling the range of turbulent dissipation energy values in the water column, and we observe that the transition zone in the southern North Sea is generally confined to water depths

* Corresponding author.
E-mail address: xdesmit@naturalsciences.be (X. Desmit).

https://doi.org/10.1016/j.scitotenv.2024.169966
Received 11 November 2023; Received in revised form 15 December 2023; Accepted 4 January 2024
Available online 10 January 2024

below 20 m. Seasonal variations in suspended particle dynamics are linked to biological processes enhancing particle flocculation, which do not affect the location of the transition zone. We identify the criteria that allow a transition zone and discuss the cases where it is not observed in the domain. The impact of these particle dynamics on coastal carbon storage and export is discussed.

1. Introduction

The dynamic nature of shelf regions is responsible for strongly fluctuating concentration patterns of suspended particulate matter (SPM). This variability is particularly pronounced within nearshore areas where fine-grained sediments are abundant. The SPM dynamics are controlled by a combination of physical and biological processes and particle characteristics (Eisma, 1986; Moulton et al., 2023). Also, SPM in a turbulent flow field is further subject to flocculation, which by changing size and excess density of the particles affect the settling velocity (e.g. Eisma, 1986). These dynamics not only depend on the concentration but also on the composition of the SPM, considering the mineral and particulate organic matter (POM) constituents (Dyer, 1989; Maggi and Tang, 2015; Maerz et al., 2016; Blattmann et al., 2019).

Despite the extensive variations in SPM concentration (SPMC), a typical feature is the persistence of a horizontal cross-shore gradient, with higher SPMCs in the shallow coastal waters and lower concentrations offshore. This cross-shore gradient in SPMC is associated with a higher POM content of SPM offshore, in contrast to a lower content found inshore (e.g. Eisma and Kalf, 1987; Jago et al., 1994). For the southern North Sea, with its tidal flats in the Wadden Sea, Postma (1984) stressed the importance of tidal asymmetries and particle trapping by density circulation and proposed the concept of a 'line of no return' located at some distance from the coast. This line would represent a boundary away from the coast beyond which any cross-transport of SPM towards the coast becomes improbable. As a consequence, POM produced nearshore tends to be processed within the coastal area and POM produced beyond the line tends to remain offshore. A nearshore utilisation and recycling of organic compounds is known to be significant when quantifying the fate of nutrient inputs from land (e.g. Asmala et al., 2017). In this perspective, only dissolved compounds (nutrients and dissolved organic matter) are exchanged across the line, which in turn may promote POM production further offshore.

From another perspective, the line of no return can be interpreted as the outer limit of a transition zone between coastal and offshore areas, which depends on the width of a surf zone of a specific depth range. Within a transition zone the aggregated particles or flocs may also exhibit maxima in sinking velocity (Maerz et al., 2016). Likewise, such a transition zone can be associated with comparable concentrations of fresh and mineral-associated POM (Schartau et al., 2019; Fettweis et al., 2022), and it may also reveal significant changes in phytoplankton order richness (Jung et al., 2017). One might thus assume that the cross-shore distribution of SPM relies, at least partially, on different hydrodynamic conditions. Moulton et al. (2023) propose that the inner shelf be the area where turbulent surface and bottom boundary layers overlap. From that perspective, the end of such overlapping could mark the transition between coastal and offshore waters, and we may expect that it affects SPM dynamics. The definition of Moulton et al. (2023), however, does not seem sufficient for some parts of the southern North Sea. For instance, the Belgian waters exhibit a cross-shore gradient in SPMC, salinity and bathymetry, while the water column remains entirely mixed in the vertical throughout the year (van Leeuwen et al., 2015). Besides, the nearshore area of the German Bight and the Seine Bay exhibit stratification due to freshwater input mainly, that weakens towards the offshore as the river plume is getting diluted by sea water (Becker et al., 1992; Brenon and Le Hir, 1999). The occurrence of salinity gradients in the nearshore results in tidal straining, which leads to a near-bottom residual current towards the coast (e.g. Simpson et al., 1990; Becherer et al., 2016; Du et al., 2022). This partially explains the persistent cross-shore gradients in SPMC found in many nearshore areas (Maerz et al., 2016). The above examples suggest that the cross-shore gradient in SPMC may occur independently of the existence of a separation between surface and bottom turbulent layers. It therefore stands to reason that there are specific sedimentological and biogeochemical processes that lead to a particular distribution in the concentration and composition of SPM, in turn influencing the transport of particles. These processes and fluxes may remain hidden or overlooked in a pure analysis of the physical conditions.

In this paper, we aim at inferring information about the transition from nearshore to offshore waters by analyzing spatio-temporal variations in the concentration and composition of SPM. We hypothesize that by disaggregating changes in the amount and composition of SPM over time and space, we can better distinguish between nearshore waters, where particles are controlled primarily by turbulence, resuspension, flocculation and deposition, and offshore regions, where variations in SPMC and composition are significantly controlled by the production and decay of plankton and detritus in the water column. Our approach applies a semi-empirical model onto field data of SPM and POM concentration from the Belgian shelf to extract POM properties (such as fresh and mineral-associated POM) along their cross-shore gradient. The model equations are then applied to remote sensing derived SPMC at the surface of the southern North Sea and the English Channel to derive the POM properties in a larger domain.

2. Methods

2.1. In situ and remote sensing data

2.1.1. In situ data

The in situ data of SPM and Particulate Organic Nitrogen (PON) concentrations have been collected between October 2004 and August 2022 on the Belgian shelf. The data set consists of hourly, 1.5 hourly or 2 hourly water samples collected during 243 tidal cycles or half tidal cycles in 12 stations, 3 of them being more sampled: one located in the nearshore coastal turbidity maximum area (MOW1, water depth about 10 m), one along the outer margin of the coastal turbidity maximum (W05; transition zone; water depth about 20 m), and the third one in the offshore area under complete Channel water influence (W08, water depth about 25 m). The amount of SPM-PON data pairs is equal to 2539. These pairs are well distributed over each month, with slightly less data in summer and autumn than winter and spring.

At every sampling occasion, three subsamples for SPMC were taken and filtered on board using pre-combusted (405 °C, 24 h), rinsed, dried for 24 h at 105 °C and pre-weighted 47 mm GF/C filters. After sampling the filters were rinsed with ultrapure water (resistivity 18.2 MΩ/cm normalized at 25 °C) and immediately stored at −20 °C, before being dried during 24 h at 50 °C and weighted to obtain the concentration. The uncertainty (expressed as the RMSE of the triplicates divided by the mean value) decreases with increasing concentration from 8.5 % (SPMC <5 mg l^{-1}) to 6.7 % (<10 mg l^{-1}), 3.5 % (10–50 mg l^{-1}) and 2.1 % (>100 mg l^{-1}) and represent the random error related to the lack of precision during filtrations. Especially in clearer water, systematic errors due to the offset by salt or other errors become much larger than the random errors (Neukermans et al., 2012). These are not included, and have been estimated based on Stavn et al. (2009) and Röttgers et al. (2014) as 1 mg l^{-1}. The samples for PON were filtered on board using 25 mm GF/C filters (pretreated as above for SPM), stored immediately at −20 °C, before being analyzed using a Thermo Finnigan Flash EA1112

elemental analyzer (for details see Ehrhardt and Koeve, 1999). The analytical uncertainty for PON is 18 % augmented with the uncertainty of the SPMC due to filtration.

2.1.2. Satellite data of SPMC

The satellite-based SPMC was generated using the Nechad et al. (2009, 2010) algorithm applied to the standard Sentinel-3/OLCI remote sensing reflectance product (RRS) provided by the EUMETSAT water processor (PB 2.00, https://earth.esa.int/eogateway/documents/20142/1564943/Sentinel-3-OLCI-Marine-User-Handbook.pdf) after applying recommended quality flags (LAND, CLOUD, CLOUD_AMBIGUOUS, CLOUD_MARGIN, AC_FAIL). While a single band can be used for SPMC estimation the optimal band depends on SPMC. If RRS is too low (e.g. for longer wavelengths in low SPMC waters) then SPMC estimation will be significantly affected by noise or errors in RRS, if it is too high (e.g. for shorter wavelengths in high SPMC waters) then the saturation phenomenon means that RRS becomes insensitive to changes in SPMC. This has led to the development of "switching single band algorithms" (Novoa et al., 2017) using the basic single band formulation of (Nechad et al., 2010) but with different wavelengths used at different SPMC and typically a smooth weighting between two adjacent spectral bands to avoid image artifacts. The Novoa et al. (2017) approach is applied to the SPMC products providing a multi-band SPMC product using two bands (red: 665 nm and near-infrared: 865 nm). Daily images of surface SPMC in the period 2017–2021 were extracted in the North Sea (lon [−4 10], lat [48 59]) with a spatial resolution of 1 km × 1 km. Daily images were then averaged to get monthly images over the same period, and data were extracted along the different transects of the study (Fig. 1).

2.2. Regional domain

The studied domain is the southern North Sea and the English Channel, with a focus on the German Bight, the Thames and East Anglia plume, the Southern Bight and the Seine Bay. The bathymetry in the domain and along four specific transects ('GE', 'UKNL', 'UKBE', 'FR') is shown in Fig. 1. The bathymetry data are gridded on a 15 arc-second geographic latitude and longitude grid, that is, any grid cell size is ~450 m on the latitude axis and ~280 m on the longitude axis (source: GEBCO 2022 Grid; see Acknowledgments). Bathymetry along the transects was smoothed with a LOESS function (span = 0.2) in MATLAB R2019a© to facilitate further interpretation.

The tides in the study area are principally semidiurnal and progress cyclonically around the North Sea, with the largest amplitudes along the coasts of the English Channel, Eastern England, the Southern Bight and the German Bight (e.g., Otto et al., 1990; Huthnance, 1991). In the central Southern Bight, the west of Denmark and the west of South Norway amphidromic points occur. The winds are variable and dominated by eastward moving depressions. The residual circulation along the North Sea coasts is cyclonic, along the English coast a southerly direction dominates up to the East Anglia coast where it turns offshore towards the northeast. Atlantic water enters the North Sea from the North and through the English Channel and the Dover Strait (Prandle et al., 1996). The freshwater inflow from the Seine, Scheldt, Rhine, Weser, Elbe and minor rivers results in coastal water masses with salinities lower than 33 and in density currents up to typically 20–40 km offshore along the southern North Sea (Prandle et al., 1997; Rijnsburger et al., 2016; Kopte et al., 2022). The SPM transport patterns in the North Sea follow the general residual current patterns and are restricted to a narrow band along the coast, except along the East Anglian coast, where

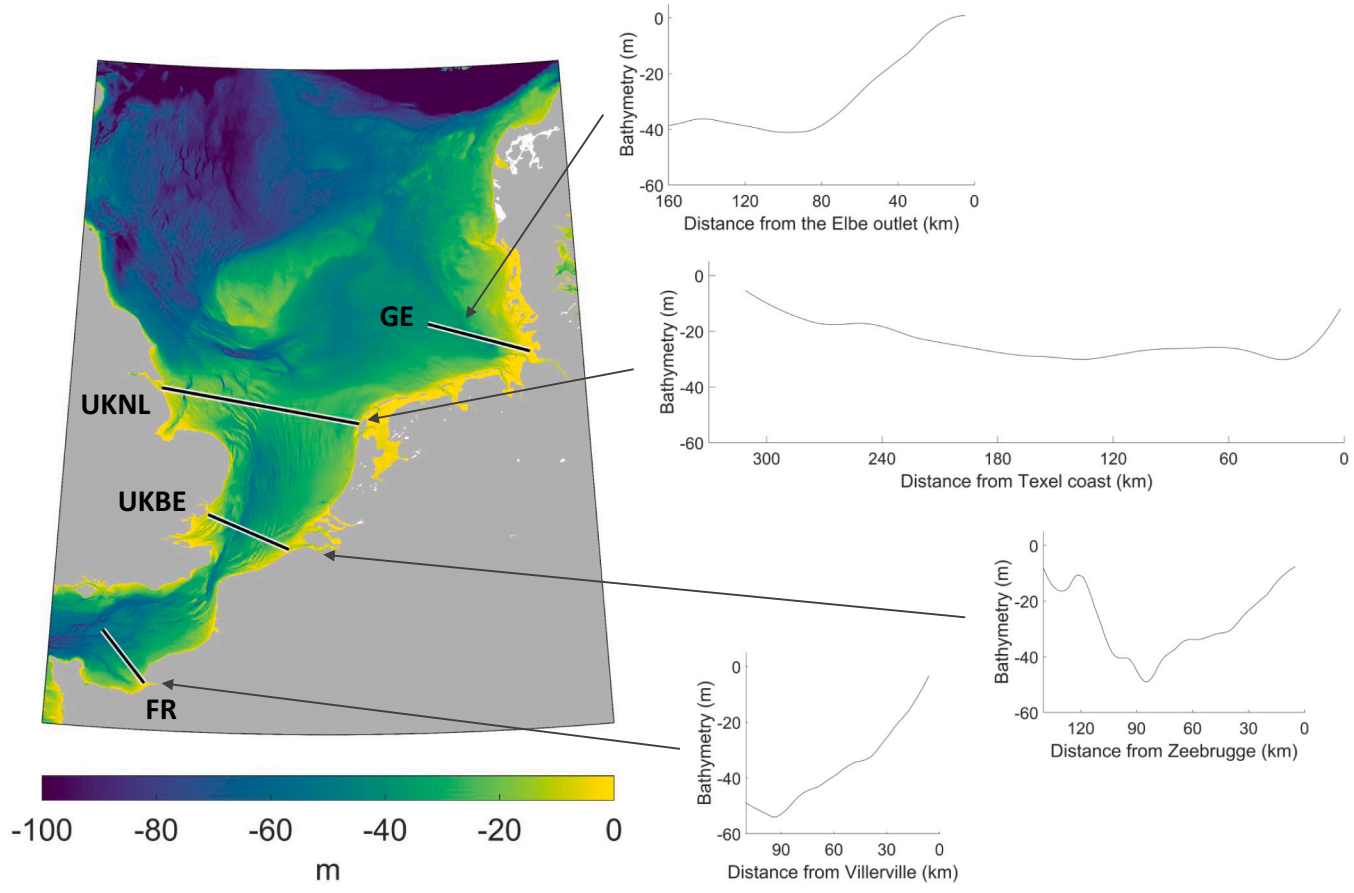

Fig. 1. Bathymetry of the southern North Sea. The black lines are showing the four transects used in this study. Side graphs on the right show the smoothed (LOESS) bathymetry along the transects.

the SPM is transported offshore towards the German Bight and the Norwegian trench (Fig. 2). The origin of the fine-grained sediments is from rivers, erosion of recent and geological layers (e.g. mud banks along the Belgian coast), coastal erosion (English Channel, east of English coast) and human impacts (see, e.g., Eisma, 1981; Dyer and Moffat, 1998; Gerritsen et al., 2001; Fettweis et al., 2009; Adriaens et al., 2018).

Satellite images show a clear difference between winter and summer SPMC, featuring a systematic decrease in summer across the continental shelf (Fig. 2). This decrease is mainly caused by the interaction between mineral and sticky exopolymeric substances that comprise organic microgels such as transparent exopolymer particles (TEP; e.g., Engel et al., 2020). During the growing season, phytoplankton excretes polysaccharides, of which a large fraction can coagulate and form TEP. This sticky TEP promotes the formation of larger flocs, enhancing the settling of the SPM (Fettweis et al., 2022). The seasonal variations in floc size and settling velocity, with higher settling rates in summer than winter, correspond well with the seasonal biological activity, whereas resuspension caused by waves, wind climate, or storms have a weaker correlation with this observed seasonality (Fettweis and Baeye, 2015).

2.3. Model of the PON content versus SPM concentration

It has been shown that the variation of the organic matter content of SPM is nonlinear and depends on the SPMC and the season (Manheim et al., 1972; Eisma and Kalf, 1987; Ittekkot and Laane, 1991). For our study we adopted the diagnostic modeling approach proposed by Schartau et al. (2019). In Fettweis et al. (2022), the usefulness of an extended model version has been documented for describing variations in particulate organic carbon and nitrogen (POC and PON), as well as for resolving changes in concentrations of transparent exopolymer particles (TEP). When calibrated with observational data, the diagnostic model can be well applied to approximate compositional changes of the SPM as a function of SPMC. In general, the POM content of SPM (POM-to-SPM ratio) changes from low to high values when SPMC decreases from highly turbid (brown) waters towards much clearer waters, respectively.

This relationship is not only observed along the inshore-offshore transect in both the German Bight and on the Belgian shelf, but also vertically between the surface and the bottom of the water column during the tidal cycle (Fettweis et al., 2022). The semi-empirical model of Schartau et al. (2019) is based on the discrimination between mineral-associated POM (POM_m), considered less reactive (Keil et al., 1994), and fresh POM (POM_f) considered more labile. The boundary condition of the model is that, when the SPMC approaches zero, the POM content of SPM converges to one, and POM is assumed to be mainly POM_f. At high SPMC, the POM content converges towards an invariant POM fraction of the SPM that is assumed to be mainly mineral-associated POM (POM_m). The remaining POM is described as a time varying fraction of the SPM, which can be attributed to the build up (primary production) and decay (remineralisation) of POM_f. Regarding the transition from highly turbid inshore towards clearer offshore waters, the relative proportion of the POM_f fraction versus the POM_m fraction increases. Accordingly, at low SPMC the POM_f fraction is high, whereas at high SPMC the POM_m fraction dominates. The same relationship can be attributed to any component of POM (e.g., POC, PON, TEP).

For our analysis we focus on the PON component of POM. The fresh fraction of the PON (PON_f) is a proxy for biomass, mainly plankton and detritus. The use of POC data would instead introduce additional uncertainties due to polysaccharide exudation and gel formation as well as physiological variations of the phytoplankton, i.e. the carbon-to-nitrogen ratio. By fitting the model to the PON data (see below), we

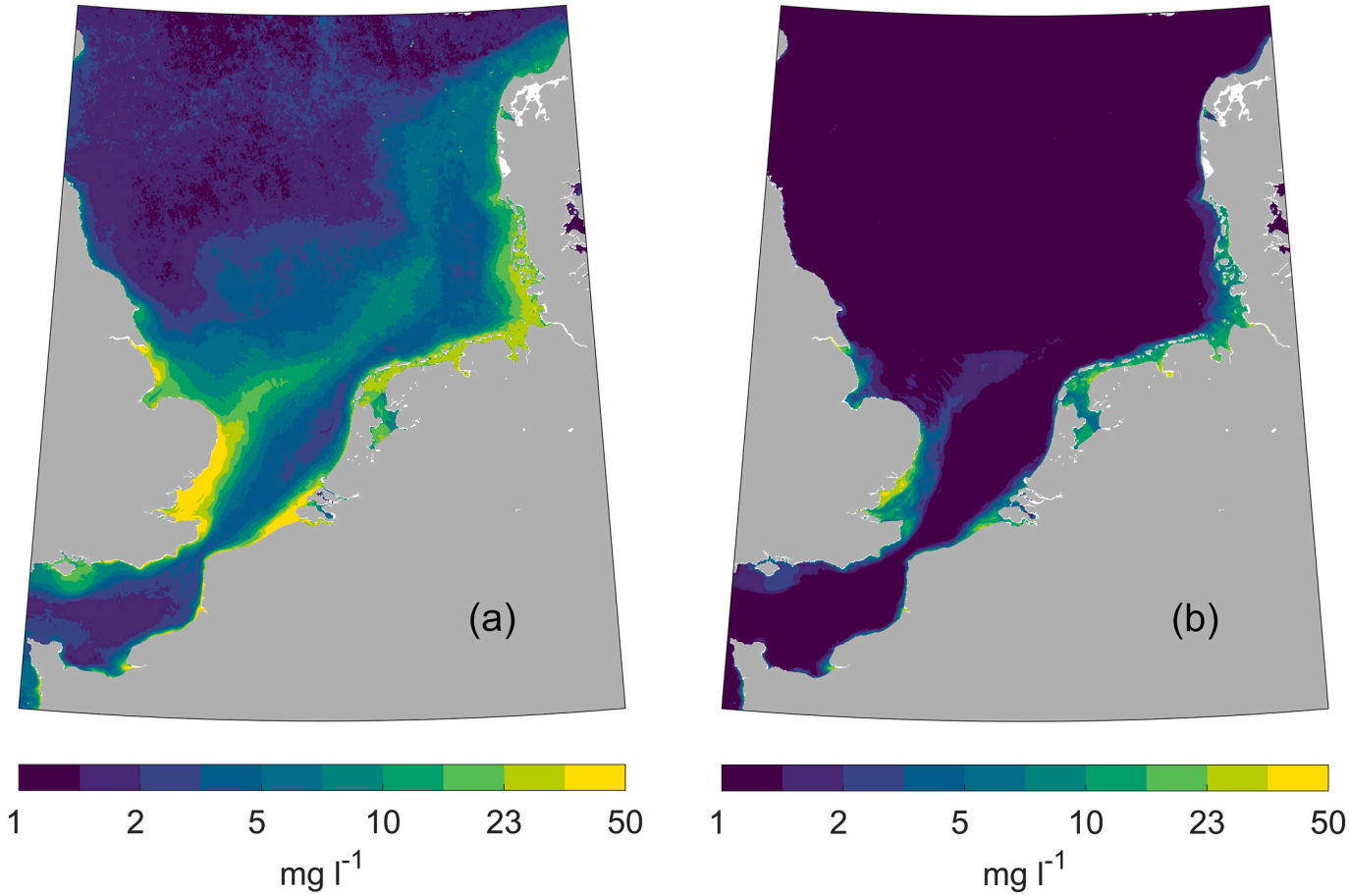

Fig. 2. Multiyear mean (2017–2021) of (a) winter (Jan, Feb, Dec) and (b) summer (Jun, Jul, Aug) surface SPMC [mg l^{-1}] in the southern North Sea.

can apply the optimized parameter values in the model (K_{POM}, $f_{1,PON}$ and $f_{2,PON}$) to recalculate the PON concentration from SPMC, while separating between the components PON_f and PON_m (Eqs. (1)–(3)):

$$PON_{modelled} = SPMC_{observed} * \frac{K_{POM} * \left(f_{2,PON} * m_{POM} + f_{1,PON}\right) + f_{2,PON} * m_{POM} * SPMC_{observed}}{\left(K_{POM} + SPMC_{observed}\right) * \left(m_{POM} + 1\right)} \quad (1)$$

$$PON_f = f_{1,PON} * \frac{K_{POM}}{\frac{K_{POM}}{SPMC_{observed}} + 1} * \frac{1}{m_{POM} + 1} \quad (2)$$

$$PON_m = f_{2,PON} * SPMC_{observed} * \frac{m_{POM}}{m_{POM} + 1}, \quad (3)$$

where m_{POM} is a factor specifying the amount of suspended POM_m along with mineral particles. Variations of m_{POM} are assumed to depend on the sediment composition (Flemming and Delafontaine, 2000), and in this study we assume m_{POM} constant (0.13) across the studied area. K_{POM} is a saturation parameter controlling the net accumulation of POM_f in the water column. Its monthly variation, thus, reflects the seasonal variation of POM_f and is assumed to be a function of available nutrients (see Schartau et al., 2019). The parameter $f_{1,PON}$ expresses the ratio of fresh PON to fresh POM (PON_f/POM_f), and $f_{2,PON}$ is the ratio of mineral-associated PON to mineral-associated POM (PON_m/POM_m), therefore, $f_{1,PON}$ and $f_{2,PON}$ are varying seasonally.

In this study, we apply the semi-empirical diagnostic model presented above to the detailed PON and SPM dataset of the Belgian shelf (Section 2.1.1) in order to derive its parameters on a monthly basis. Best model representations of the PON:SPM data were obtained by identifying model parameter values that minimize a cost function that includes the sum of squared data-model residuals divided by the respective observational errors (variances). When considering these weighted least squared misfits only, a collinearity exists between estimates of the parameters $f_{1,PON}$ and K_{POM}, in particular when individual subsamples yield estimates of K_{POM} below 0.5 mg l^{-1}. To overcome this difficulty, a Gaussian-based prior is added to the weighted least square misfit, imposing a K_{POM} value of 2 mg l^{-1} with a 100 % uncertainty. Such extension of the cost function ensures that the optimization problem is well-defined, leading to robust parameter estimates. To identify the optimal combinations of the three model parameters, we systematically explored the three-dimensional manifold of the cost function. Rather than applying an optimization algorithm, this is simply achieved by evaluating cost function values for a three-dimensional array of parameter combinations. The element of this array with the lowest cost function value represents the best combination of parameter values. The array's individual dimensions cover the variational range for $f_{1,PON}$, $f_{2,PON}$, and K_{POM}, respectively. For $f_{1,PON}$ the interval between $[10^{-3}, 1]$ is covered with a resolution of $\Delta = 10^{-3}$, and for $f_{2,PON}$ the interval covers $[5 \times 10^{-4}, 1]$ with $\Delta = 10^{-4}$. To account for the wide range of possible values for K_{POM}, spanning two orders of magnitude, we implemented a constant resolution on a logarithmic scale within the interval $\log_{10}(K_{POM}) \in [\log_{10}(0.1), \log_{10}(10)]$. This logarithmic scale approximation aims to achieve a precision of approximately 1 %.

The model is, then, applied pixel wise to the satellite SPMC images (Section 2.1.2) in the southern North Sea, assuming the same model parameters for all areas (see Eqs. (1) to (3)). This provides qualitative information on SPM composition, in addition to the original SPMC levels, in order to investigate the coastal-to-offshore patterns of SPM dynamics.

3. Results

3.1. Model-based estimates of PON_f and PON_m

The SPM composition, more specifically its PON fraction, changes in a characteristic way with SPMC. A progressive increase of the PON fraction occurs with decreasing SPMC from nearshore to offshore waters (Fig. 3).

The PON content increases in the spring and summer (Fig. 3 c-g) while phytoplankton blooms and detritic particles accumulate in the bulk, until the fall and winter when heterotrophic processes dominate. Also, the general decrease in SPMC during summer (May–August) compared to the winter period is observable in these graphs (distribution around lower values on the horizontal axis). The model was fitted against the data, reproducing the cross-shore gradient and the seasonal trend, and providing monthly model estimates for its parameters (Table 1). Statistics shown in Table 1 indicate the goodness of fit. The Root Mean Square Error (RMSE) is expressed in the units of PON:SPM and should be small. The normalized cost function would be equal to 1 if the data-model misfit was perfect. While the RMSE does not account for uncertainties in observations, the cost function (weighted least squares) does and thus provides more meaningful assessment of the model fit. The range of uncertainty of the fit increases towards low SPMC due to the lack of data constraints (e.g., February in Fig. 3b). This does not necessarily prevent good model representations of the available observations, as shown by corresponding statistics. Overall, only for June, July and October the model estimates reveal a less good fit to observations. The model parameters allow calculating a modelled PON concentration from the SPMC, and also the fractions PON_f and PON_m (Eqs. (2) and (3)). The values of Table 1, generated by fitting the model on the available Belgian data, are applied to all transects in this study, assuming they are representative of North Sea particle dynamics.

3.2. Multiyear mean winter and summer PON concentration in the North Sea

Using the model's best parameter estimates, we derived PON, PON_m and PON_f concentrations from SPMC and applied it pixel wise to the satellite images in the southern North Sea and the English Channel. The uncertainties in the model parameters enhance the errors of the pixel wise values for POM_f and POM_m in comparison with the satellite SPMC they are derived from. However, for geographical entities, which extend over tens of kilometers and comprise a larger number (10 to 100) of pixels, they still reveal robust patterns. We use ΔPON, the difference between PON_m and PON_f concentrations (PON_m - PON_f), to highlight the spatio-temporal variations of the PON dynamics and composition. It is shown for the months of January 2020 at Fig. 4a and April 2020 at Fig. 4b.

ΔPON varies in time and space as both fractions PON_m and PON_f undergo biogeochemical transformations. In winter, ΔPON shows the highest values at the coast due to the dominance of PON_m and rapidly decreases towards the offshore, where values are typically closer to zero as both PON_m and PON_f are low and closer in concentration (Fig. 4a). A notable exception offshore is the turbid Thames River plume carrying SPM from East Anglia across the sea to the German Bight and the coast of Denmark, and where PON_m dominates. In the spring (Fig. 4b), ΔPON shows its minimum values in a narrow area close to the coast. In that area, the freshly produced fraction of PON in spring is found in higher

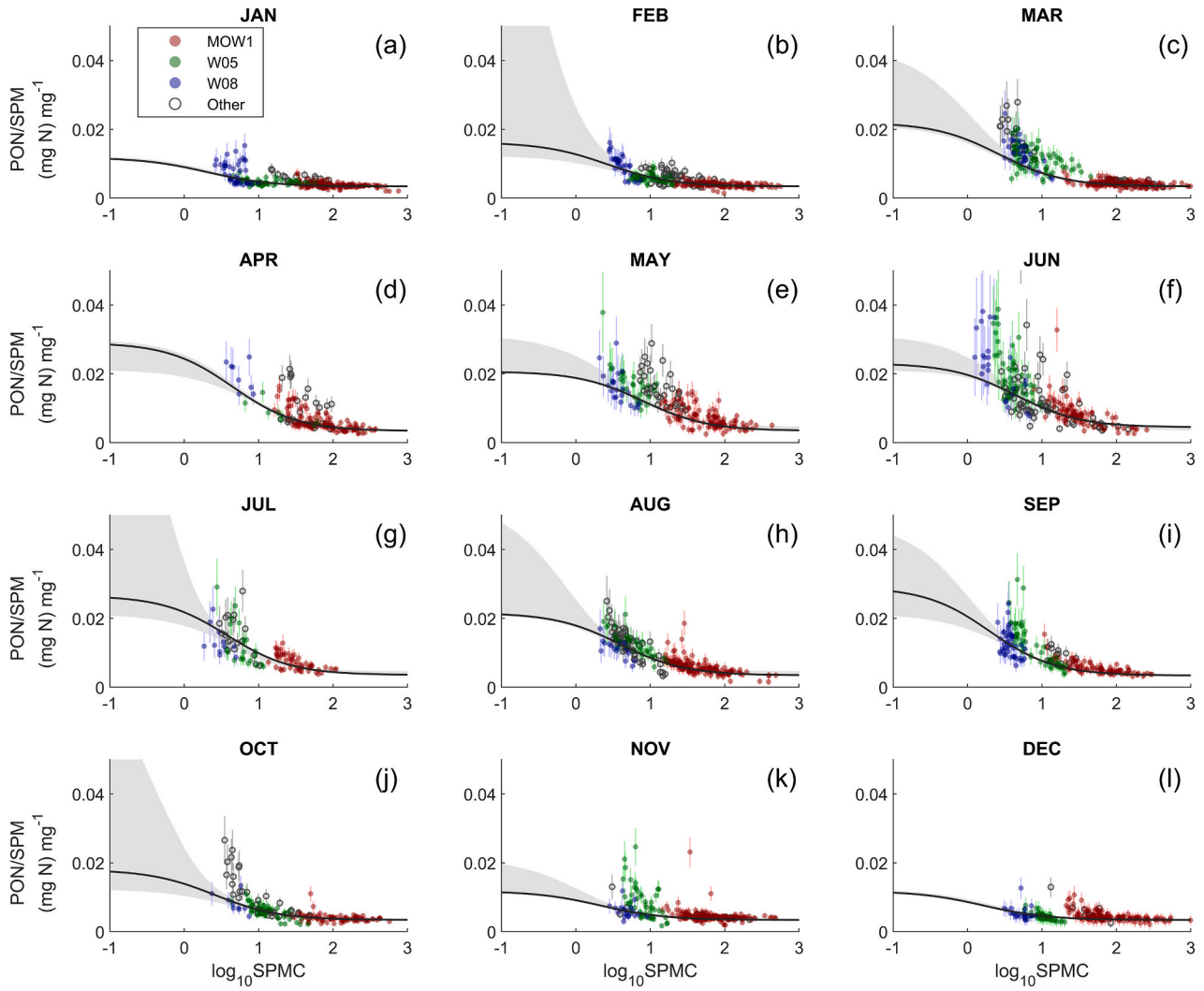

Fig. 3. PON content of SPM [(mg N) mg^{-1}] as a function of SPMC, in situ monthly data sampled at twelve stations along the coastal-offshore gradient on the Belgian shelf. Three stations have been relatively more sampled: MOW1, W05 and W08 (see legend for colours). The black line represents the model fit, and the grey area represents the uncertainty envelope (at the 95 % confidence interval).

Table 1
Monthly model parameters and associated statistics obtained from model fitting for the PON content of SPM along the coastal-offshore gradient on the Belgian shelf.

Month	PON: fitting parameters			Statistics	
	K_{POM}	$f_{1,PON}$	$f_{2,PON}$	RMSE	Cost function
	mg l^{-1}	(mg N) mg^{-1}	(mg N) mg^{-1}	(mg N) mg^{-1}	–
Jan	2.00	0.0095	0.0295	0.0016	1.02
Feb	2.66	0.0145	0.0295	0.0014	1.12
Mar	2.68	0.0210	0.0295	0.0035	1.40
Apr	4.47	0.0290	0.0295	0.0035	1.70
May	8.00	0.0195	0.0300	0.0044	1.73
Jun	4.46	0.0210	0.0390	0.0119	2.10
Jul	3.77	0.0260	0.0310	0.0037	3.19
Aug	3.90	0.0205	0.0300	0.0024	0.88
Sep	1.99	0.0290	0.0295	0.0036	1.23
Oct	2.55	0.0165	0.0295	0.0030	2.29
Nov	2.13	0.0095	0.0295	0.0030	1.78
Dec	1.63	0.0095	0.0295	0.0026	1.80

concentrations than the mineral-associated PON, which leads to negative values of ΔPON. While PON_f concentration in spring is a proxy for phytoplankton biomass, PON_m always reflects the mineral fraction of SPM, which predominantly originates from resuspended sediment particles.

3.3. Monthly variation of PON along cross-shore transects

The monthly variations of PON_f and PON_m have been calculated for the four selected transects. The resulting ΔPON features a high seasonal variability, which is illustrated for the transect 'GE' in Fig. 5c (see Appendix A for the other transects). PON_f is linked to seasonal photosynthesis and organic matter degradation processes. Therefore, PON_f concentration is low in winter and increases during spring and summer in relation to the bloom and post-bloom processes. It decreases in the fall when heterotrophic processes dominate the phototrophic processes. PON_m concentration is proportional to the mineral particle concentration. Therefore, it exhibits a decrease from winter to summer and an increase in the fall, following the seasonal cycle of SPMC (see Section 2.2; Fig. 2). At any time of the year, both PON_m and PON_f show higher concentrations at the coast than offshore. Such a cross-shore difference becomes much less significant for PON_f in winter when plankton growth is minimal. During the growing season, PON_f reaches the highest

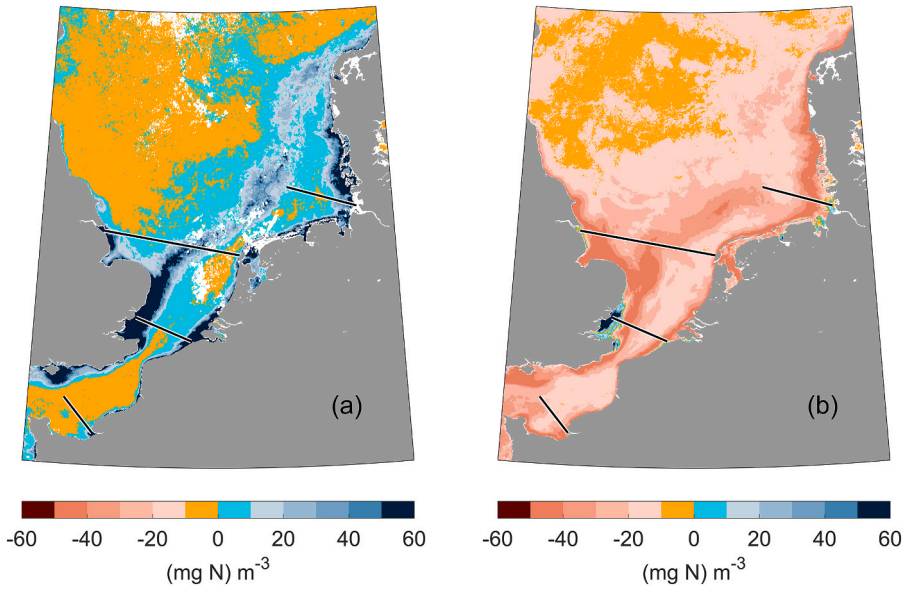

Fig. 4. Surface ΔPON (PON_m-PON_f) concentration [(mg N) m^{-3}] in 2020, January (a) and April (b). Black lines are the transects of interest (see Fig. 1).

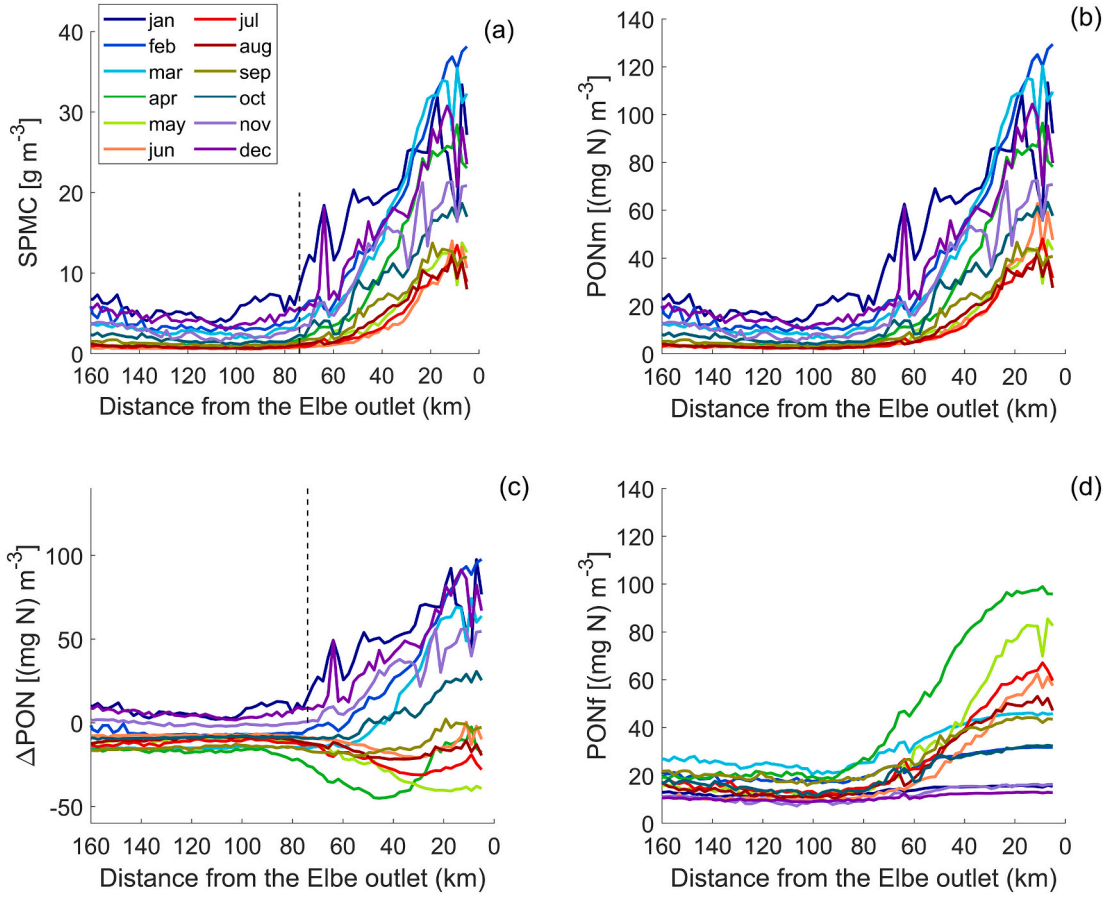

Fig. 5. Monthly surface (a) SPM, (b) PON_m, (c) ΔPON and (d) PON_f concentrations along the transect 'GE' (satellite-derived data). Each line represents the multi-year mean values for one month in the period 2017–2021. The dashed vertical line corresponds to the location where ΔPON reaches its offshore value (see text).

concentrations, especially in April and May at the coast and in March, April and September offshore.

As a result of the seasonal variability of PON_f and PON_m, ΔPON follows a coastal-offshore gradient similar to the one of PON_m during winter months. This cross-shore gradient is characterized by a strong decrease in concentration between the coast up to ~75 km from the Elbe outlet. In the spring and summer, during a period of an increase in PON_f while PON_m decreases, the resulting ΔPON is characterized by lower values (mostly negative values) across the transect. ΔPON shows minimum values from April to September between the coast and ~75 km

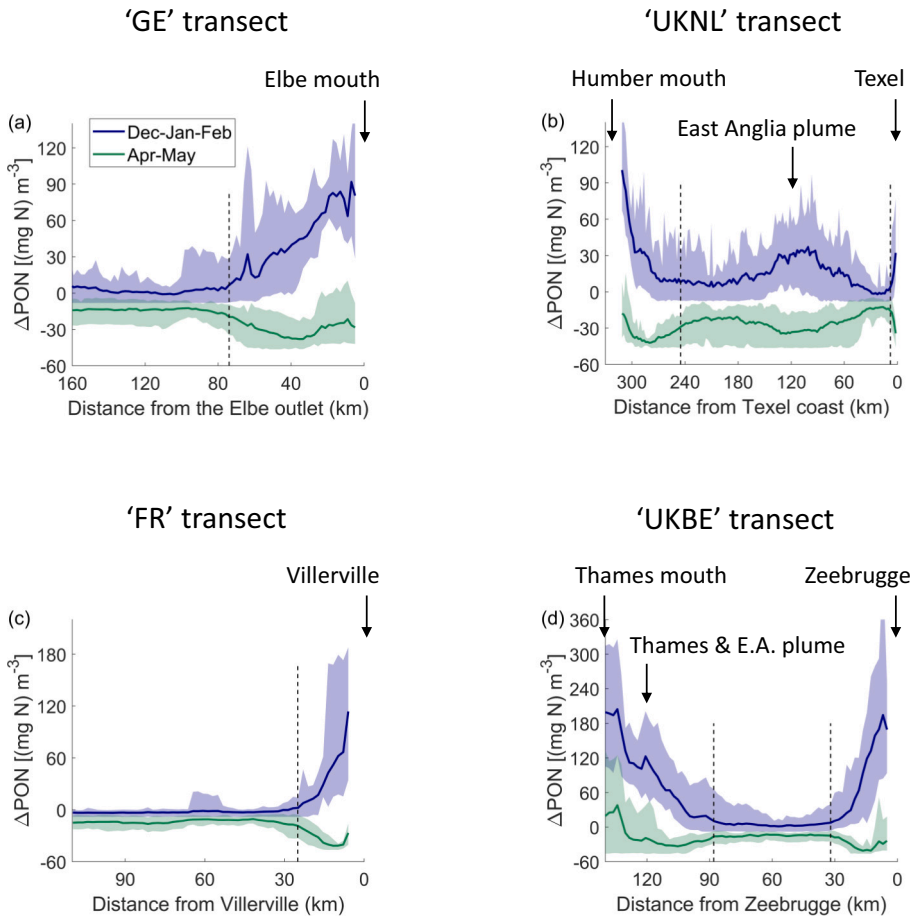

Fig. 6. Surface ΔPON (PON_m-PON_f) concentration [(mg N) m^{-3}] in winter and spring along four transects (a. 'GE' transect; b. 'UKNL' transect; c. 'FR' transect; d. 'UKBE' transect). Lines show the multiyear mean values (2017–2021) and shaded areas illustrate the multiyear minimum and maximum values. The dashed vertical lines correspond to the locations where ΔPON reaches its offshore value (see text).

offshore from the Elbe outlet. In April, when phytoplankton production is at its highest, more negative values of ΔPON occur between km 20 and km 75 from the Elbe outlet. In that zone, although PON_f shows lower concentrations than at the coast, the PON_m concentration has dropped to such an extent that ΔPON reveals its lowest value. This characteristic seems to be a robust feature for many coastal regions, and exceptions or deviations suggest some underlying dynamics, in particular with respect to the cross-shore transport of SPM, that differs from other areas. Over the entire North Sea, such a zone of lowest ΔPON is visible as the dark red narrow area on Fig. 4b, where ΔPON<-40 (mg N) l^{-1}. Typically, it is found as an alongshore feature.

Fig. 6 shows the average winter (blue) and spring (green) ΔPON profiles over the four studied transects. The main characteristics of ΔPON variability across the 'GE' transect are also observable in other coastal zones, whether featuring low turbidity like the Texel coast ('UKNL' transect), moderate turbidity like the Seine Bay ('FR' transect) and the Humber mouth (north of East Anglia; 'UKNL' transect), or high turbidity like the Belgian coast and the Thames mouth (south of East Anglia; 'UKBE' transect). In winter, ΔPON is dominated by PON_m and reflects well the SPMC. In spring, PON_f concentration increases due to biological activity while PON_m decreases concomitantly due to TEP accumulation in the bulk and settling of the flocs, which results in a considerable decrease in ΔPON at the coast (towards negative values). As ΔPON is derived from satellite SPMC, the East Anglia plume and the Thames plume are visible respectively in the 'UKNL' and 'UKBE' transects, especially in winter. The fact that the East Anglia plume is visible in satellite images in winter suggests that the particles have low settling velocities due to their small grain sizes. It is the lateral transport of particles from the Thames that is responsible for the extensive cross-shore spread of SPM, since it is unlikely that particles from the bottom be resuspended towards the surface along the trajectory of the plume, especially when bathymetry increases. Clearly, the other coastal areas, including river mouths and estuaries, do not reveal a similar cross-shore spreading of SPM. In spring, the East Anglia plume is also visible with lower values of ΔPON compared to surrounding waters, which suggests a higher phytoplankton production in the plume. Along the coastal-offshore transects, the annual variability of ΔPON (shaded area in Fig. 6) is lower than the spatial and seasonal variability in the period 2017–2021, suggesting that basin morphology and seasonal processes, such as phytoplankton production, mainly control the particle dynamics. This tends to be less obvious in offshore waters.

3.4. Variations of PON with regard to bathymetry

So far we looked at variations in ΔPON along cross-sections with regard to the distance from the coast. Despite predominant features being similar, the distances at which the spatial gradients in the variation of ΔPON approach their minimum remain elusive. In order to test the dependency of ΔPON on basin morphology, ΔPON can also be represented as a function of the bathymetry along the transects (more specifically along each coastal-offshore sub-transects; Fig. 7). In most of our studied cases, the winter decrease in ΔPON occurs within bathymetry below ~20 m, and likewise in spring we find the trough in ΔPON to occur within the same depth range, with the exceptions of the Elbe and Thames cases where it occurs, respectively, within bathymetry 5–35 m (Fig. 7a) and 15–50 m (Fig. 7d). It should be pointed out that in spite of

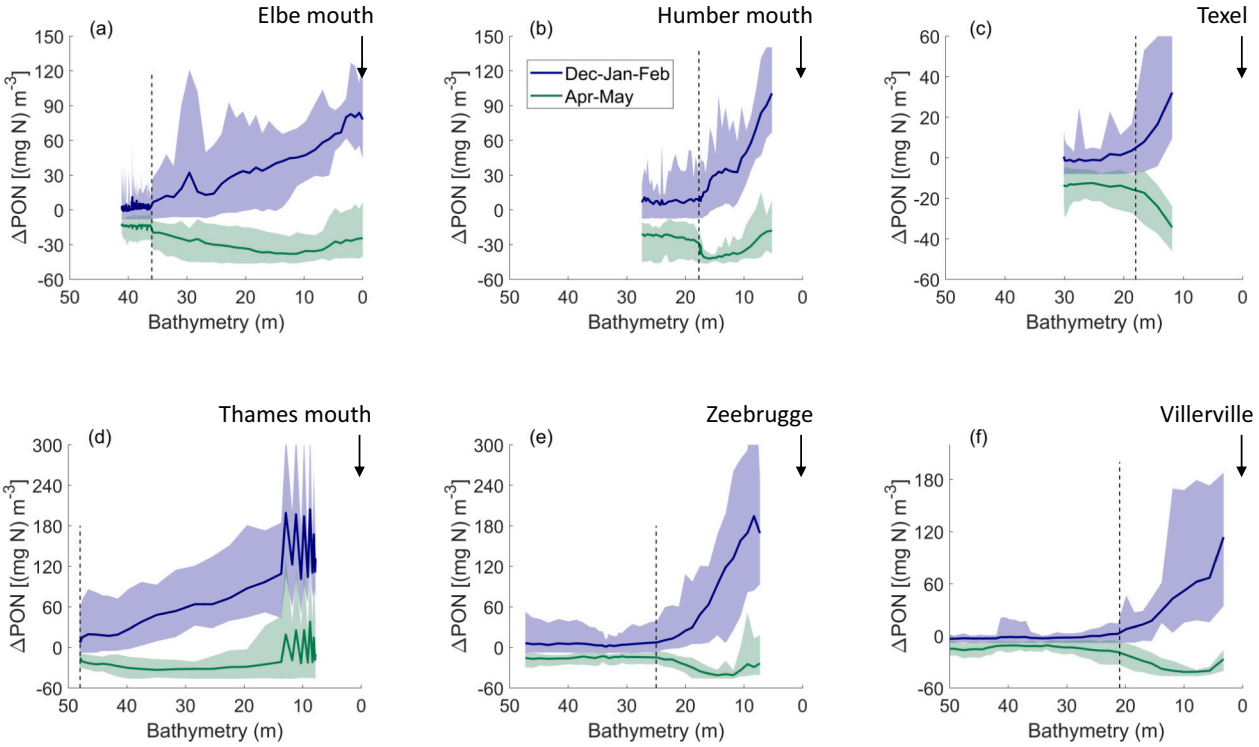

Fig. 7. Surface ΔPON (PON_m-PON_f) concentration [(mg N) m^{-3}] in winter and spring as a function of bathymetry (a. 'GE' transect; b. 'UKNL' transect, Humber plume; c. 'UKNL' transect, Texel coast; d. 'UKBE' transect, Thames plume; e. 'UKBE' transect, Belgian coast; f. 'FR' transect). Lines show the multiyear mean values (2017–2021) and shaded areas illustrate the multiyear minimum and maximum values. The dashed vertical lines correspond to the locations where ΔPON reaches its offshore value (see text).

the complexity of particle dynamics in coastal zones, ΔPON values tend to stabilize in most cases around bathymetry 20 m (or 35 m in the Elbe case; Transect 'GE'), where ΔPON reaches its offshore value while its winter and spring annual variabilities tend to overlap. Also, beyond bathymetry 20 m, the SPM dynamics generally adopt an offshore regime (Fig. 5a and Figs. A.1, A.2, A.3). These results suggest that bathymetry 20–35 m be the location of the virtual 'line of no return', which may also depend locally on river plume dynamics.

4. Discussion

The transition zone between coastal and offshore waters was investigated along four transects as a function of the distance to the coast. We define the transition zone as the part of the coastal area where the ΔPON in April–May (Fig. 6) shows a trough, i.e., where PON_f mostly dominates PON_m. Along the continental coast, it roughly occurs between 20 and 75 km from the Elbe outlet in the GE transect (Fig. 6a), within the first 8 km offshore Texel (Fig. 6b), between 5 and 25 km from Villerville in the Seine Bay (Fig. 6c), and between 10 and 30 km from Zeebrugge in the BE transect (Fig. 6d). It was also represented as a function of bathymetry because of the indirect, though central, influence of the latter on particle dynamics (see below in §4.1). The defined transition zone is located in 4 of the 6 transects shown at Fig. 7 between ~5–20 m water depth. Exceptions are the Thames mouth, where an overlap with the East Anglian plume may distort the pattern, and the Elbe plume, which extends along its Glacial Valley and is not representative, in this respect, of the rest of the German Bight. Beyond the studied transects, the transition zone tends to occur within depths below 20 m in the southern North Sea and the English Channel, as shown in Fig. 8. This zone corresponds to an area where turbulence is decreasing and the settling velocity has a local maximum, as Maerz et al. (2016) derived for the German Bight. In the case of the transition zone overlapping with a region of freshwater influence, the net transport of settled particles during a tidal cycle is directed towards the coast due to ebb-flood asymmetries in the vertical profile (Becherer et al., 2016). These processes cause a net accumulation of particles in the coastal zone (Postma, 1981), shaping the strong horizontal gradients of SPMC. From our point of view, the offshore outer limit of the transition zone (corresponding to a bathymetry of ~20 m) represents the 'line of no return' as put forward by Postma (1984).

4.1. Effect of bathymetry on particle dynamics

Turbulence is a major factor controlling the resuspension and settling of fine-grained particles. Turbulence is due to wind and the tidal dynamics, which cause shear stresses at the surface and bottom boundaries of the water column. While lower levels of turbulence permits flocculation in turbid areas, where the collision probability remains significant, high levels of turbulence will result in floc breakup, leading to a higher number of smaller particles. In addition to the density of particles, the median size of particles is key to predict their settling rates as smaller particles show lower downward flux due to the water viscosity that reduces their terminal velocity. In contrast, larger particles exhibit a higher net downward mass flux. Bathymetry controls the propagation of turbulent kinetic energy between the surface and bottom boundaries of the water column. Bathymetry is therefore a controlling factor determining the median particle size in the water column through floc formation/breakup, and it also determines whether resuspended particles may reach the surface. In shallow waters, there is typically an increased shear stress on the sediment that enhances resuspension of particles. As is known, this effect decreases with increasing water depth, up to the point where the resuspended particles only remain in the lower layers near the bottom. Overall, the net downward flux of particles depends on the vertical profiles of water viscosity and turbulence as well as on the particles' size structure and excess density. These particle properties change with flocculation, which in turn depends not only on the turbulence but also on the abundance and composition of the SPM (Ho et al., 2022; Yu et al., 2023).

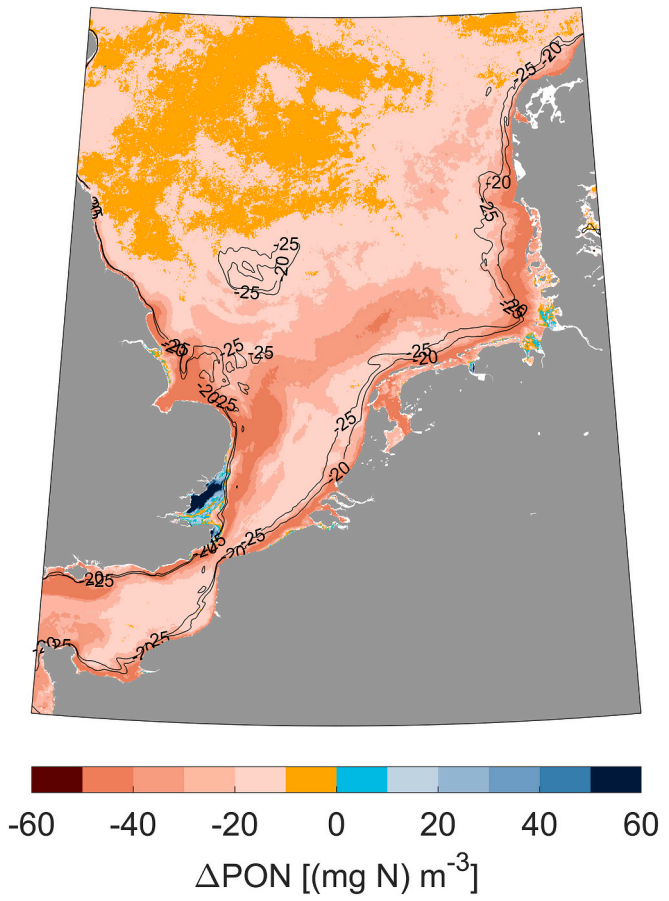

Fig. 8. Surface ΔPON (PON_m-PON_f) concentration in April 2020 with isolines (black) of bathymetry 20 m and 25 m.

4.2. SPM and POM storage and export

Some hypotheses can be made on the influence of the transition zone on SPM and POM storage and export. The well pronounced seasonal variability in PON_f is mainly due to phytoplankton production, whereas the variability seen in PON_m can be attributed to variations in the amount of resuspended matter or the settling behavior of the particles, as, for instance, an increased averaged settling of particles during the growing season due to more effective flocculation. In the case of the German Bight (transect 'GE'), the most upstream values of PON_f concentration increase by ~80 (mg N) m^{-3} (~15–20 (mg N) m^{-3} offshore) between December and April (March, offshore), illustrating the size of the spring bloom (Fig. 5d). Concomitantly, PON_m concentrations decrease by ~100 (mg N) m^{-3} (~13–17 (mg N) m^{-3} offshore) between the end of the winter and the summer, which can be explained by an increase in particle settling in response to the increase in median floc size from the winter to the summer (Fettweis et al., 2022). Even in the absence of any hydrodynamical process responsible for keeping the particles at the coast, several processes can be identified that limit the export of fresh POM to the offshore. In front of the Belgium coast, in winter, when the fresh and sticky components of EPS, including TEP, are found in negligible concentrations in the water column, the SPM remains an assemblage of fine-grained particles, with median floc sizes of ~50–60 μm on average during a tidal cycle (Fettweis and Baeye, 2015). These flocs are deposited and resuspended at tidal scale and, thus, a long-term deposition in the benthic layer is unlikely to occur. During spring and summer, while the fresh and more sticky TEP is accumulating in the bulk, the particles tend to form flocs with median sizes of ~80–150 μm on average during a tidal cycle. A significant part of the SPM settles and remains on the seabed with a lower probability of being resuspended during the tidal cycle than in the winter (Fettweis and Baeye, 2015). As particles settled on the seabed do not move significantly compared to particles in suspension, the increased particle settling in summer also diminish the horizontal transport of SPM and POM. In that sense, the seasonal vertical processes influence the range of the horizontal dispersal of SPM and POM. The line of no return is an emergent property of systems where particles are subject to these coupled vertical and horizontal processes. From a literal point of view, the line of no return inhibits the SPM transport from coastal to offshore waters. We note that this does not exclude a residual, albeit small, net flux of fresh POM produced offshore towards the coast.

Thus, we may hypothesize that a transport of particles is possible between coastal and offshore waters, but it is limited. Such transport is more important during the winter when floc sizes and settling rates are lower, and it is also correlated with the export of mainly mineral-associated POM. In spring and summer, when the SPM is enriched in fresh POM, it is also more subject to local sedimentation and trapping into the benthic fluffy layer. As a consequence, the fate of fresh and mineral-associated POM is different. While fresh POM produced in the coastal zone tends to remain there, the mineral-associated POM may be subject to transport towards the offshore to be eventually stored in the open ocean, predominantly in winter. The remineralization of fresh POM in the coastal zone enriches the system with dissolved nutrients. Those can be locally uptaken or transported away since dissolved substances are not limited by the line of no return (Postma, 1984).

4.3. Criteria for a transition zone in the North Sea

The concept of transition zone as described above, is based on several conditions: elevated SPMC, tidal hydrodynamics that generate strong alongshore and weak cross-shore currents, horizontal salinity gradients (freshwater input), and an area of increased settling velocities controlled by turbulence values that enhance flocculation (bathymetry dependent). Areas that fit these criteria are the east coast of England down to East Anglia, the southeastern coast from the Dover Strait up to the German Bight and Denmark, and the Seine Bay (Fig. 8). In these areas, a strong cross-shore gradient of SPMC is observed. Areas that do not fulfill all these criteria are the southern coast of England from the Isle of Wight up to East Anglia, the Somme Bay and the North Holland coast. In these areas, the cross-shore particle transport mechanism differs from those where the apparent line of no return largely corresponds to the 20 m isobath. The SPM plume offshore the East Anglia coast is not confined to the coast and stretches out across the southern North Sea up to the German Bight. The direction of the strong cross-shore currents corresponds to the flow fields of the cyclonic tidal wave and the inflow of Atlantic waters through the Dover Strait. The area of the Isle of Wight, although rich in SPM, is not subject to significant freshwater input and, thus, hydrodynamical processes keeping the particles at the coast are presumably small. Consequently, the coastal-offshore pattern of SPMC greatly exceeds the 20 m isobath. The Somme Bay exhibits neither high SPMC nor a significant density gradient. The North Holland coast has low SPMC at the surface. However, the influence of the Rhine ROFI may locally perturbate the vertical density gradient, and additionally may cause an underestimation of satellite-derived SPMC (Pietrzak et al., 2011).

5. Conclusion

Coastal areas with elevated SPMC, and with strong alongshore, weak cross-shore currents, and horizontal salinity gradients, feature a land-ocean transition zone that can be identified based on temporal and compositional changes of the particles. Spatial and seasonal variabilities dominate the particle dynamics, suggesting that basin morphology and biological activity mainly control the processes at play. Bathymetry plays an important role in determining the turbulence effects on the flocculation and settling of particles. Our study shows that the coastal

SPMC maximum and thus the maximum settling of particles generally occurs within depths below 20 m. Generally, the seasonal production of phytoplankton should enhance the particle settling and thus the accumulation of freshly produced particles at the bottom during the summer period. Due to vertical and horizontal density gradients and hydrodynamic (tidal) forcings, the particles in the transition zone may become subject to a near-bottom net transport towards the coast, hence maintaining the cross-shore gradient of particles. The offshore limit of the transition zone can thus be regarded as the 'line of no return' put forward by Postma (1984) across which any transport of SPM and its organic matter components becomes small throughout the year, especially in the growing season. The dynamics of particles in the transition zone have an effect on the fate of organic matter. The freshly produced POM and a substantial part of the mineral-associated POM tend to remain in the shallower areas of the coastal waters, while a minor fraction of the mineral-associated POM is exported to the offshore during the winter. The impact of such particle dynamics on the carbon and nitrogen cycles in shelf seas could be further quantified in the future with modeling tools.

Funding section

The research was supported by the Belgian Science Policy (BELSPO) within the BRAIN-be programme (BG-PART, contract nr B2/202/P1/BG-PART, and PiNS, contract nr RV/21/PiNS), the Maritime Access Division of the Flemish Ministry of Mobility and Public Works (MOMO project), and the RBINS BGCMonit program. Scientific input from Markus Schartau and Rolf Riethmüller are integrated in the research topics "Marine and polar life" and "Coastal zones at a time of global change" of the project-oriented funding programme: Changing Earth - Sustaining our Future, funded by the Helmholtz Association of German Research Centers.

CRediT authorship contribution statement

Xavier Desmit: Conceptualization, Data curation, Formal analysis, Funding acquisition, Investigation, Methodology, Project administration, Resources, Software, Supervision, Validation, Visualization, Writing – original draft, Writing – review & editing. **Markus Schartau:** Conceptualization, Formal analysis, Investigation, Methodology, Software, Writing – original draft, Writing – review & editing. **Rolf Riethmüller:** Conceptualization, Investigation, Methodology, Supervision, Writing – review & editing. **Nathan Terseleer:** Conceptualization, Formal analysis, Methodology, Software, Supervision, Visualization, Writing – review & editing. **Dimitry Van der Zande:** Data curation, Formal analysis, Funding acquisition, Methodology, Software, Visualization, Writing – review & editing. **Michael Fettweis:** Conceptualization, Data curation, Formal analysis, Funding acquisition, Investigation, Methodology, Project administration, Resources, Supervision, Validation, Writing – original draft, Writing – review & editing.

Declaration of competing interest

To their best knowledge, the Authors do not have any actual or potential conflict of interest including any financial, personal or other relationships with other people or organizations within three years of beginning the submitted work that could inappropriately influence, or be perceived to influence, their work.

Data availability

Data used in this study (in situ concentrations, bathymetry) are available online. See Acknowledgements section for references.

Acknowledgements

Ship time with the RV Belgica was provided by BELSPO and RBINS-OD Nature. The SPM and POC analysis have been done in RBINS's ECOCHEM Laboratory. Data of in situ SPM and PON concentrations are freely available on request at https://www.bmdc.be/NODC/search_data.xhtml. Bathymetry information and images were derived from GEBCO Compilation Group (2022), GEBCO 2022 Grid (doi:https://doi.org/10.5285/e0f0bb80-ab44-2739-e053-6c86abc0289c). Maps were performed in Matlab with M_Map (Pawlowicz, 2020).

Appendix A

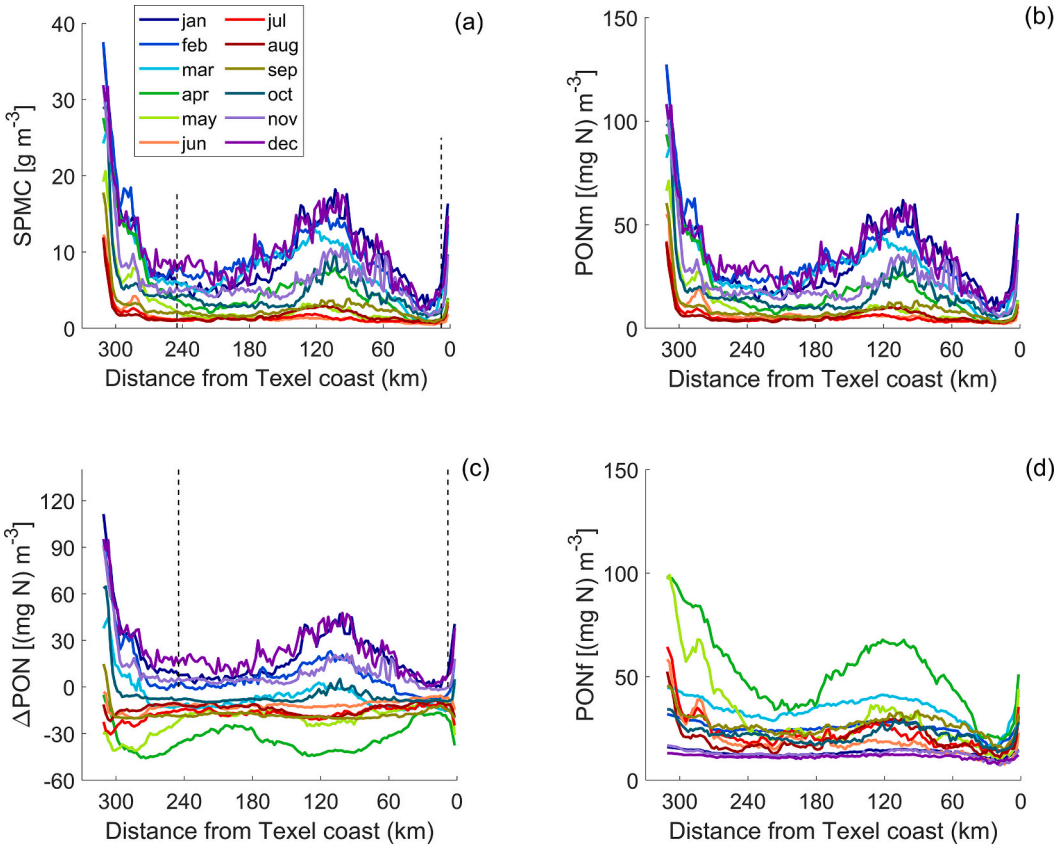

Fig. A.1. Monthly surface (a) SPM, (b) PON_m, (c) ΔPON and (d) PON_f concentrations along the transect 'UKNL' (satellite-derived data). Each line represents the multi-year mean values for one month in the period 2017–2021. The dashed vertical lines correspond to the locations where ΔPON reaches its offshore value (see text).

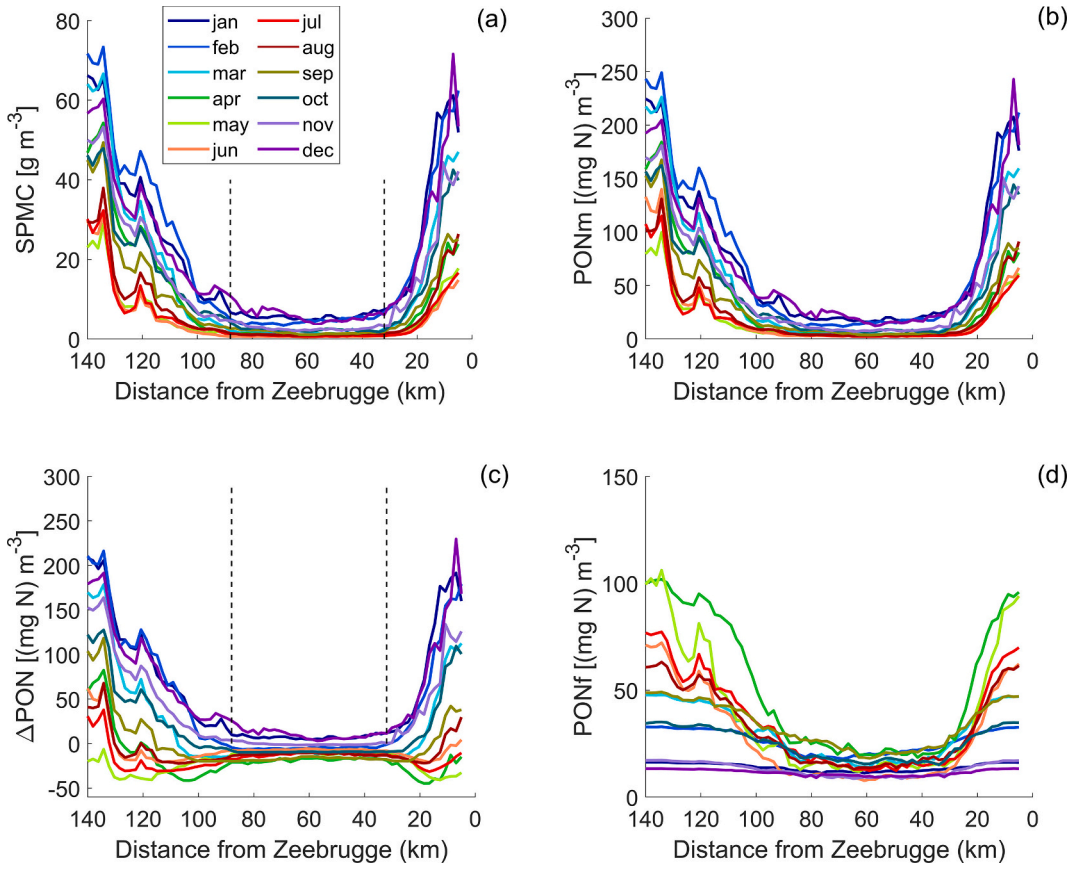

Fig. A.2. Monthly surface (a) SPM, (b) PON_m, (c) ΔPON and (d) PON_f concentrations along the transect 'UKBE' (satellite-derived data). Each line represents the multi-year mean values for one month in the period 2017–2021. The dashed vertical lines correspond to the locations where ΔPON reaches its offshore value (see text).

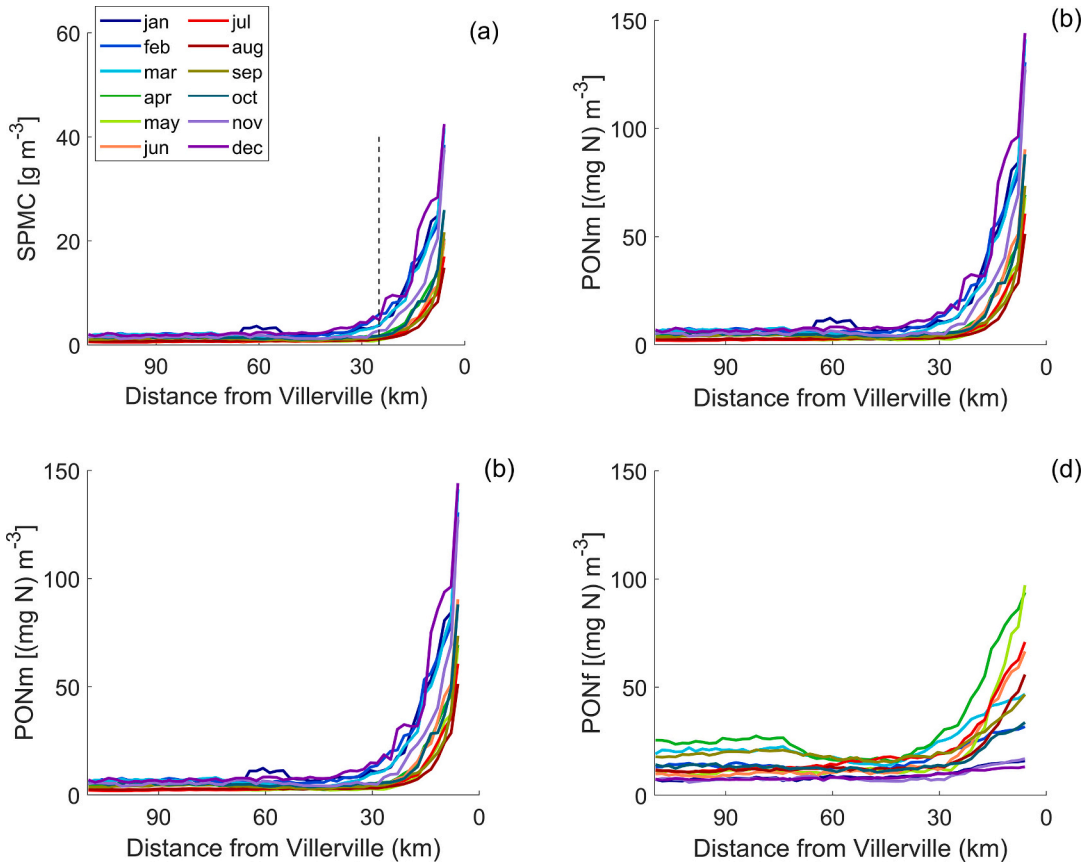

Fig. A.3. Monthly surface (a) SPM, (b) PON_m, (c) ΔPON and (d) PON_f concentrations along the transect 'FR' (satellite-derived data). Each line represents the multi-year mean values for one month in the period 2017–2021. The dashed vertical line corresponds to the location where ΔPON reaches its offshore value (see text).

References

Adriaens, R., Zeelmaekers, E., Fettweis, M., et al., 2018. Quantitative clay mineralogy as provenance indicator for recent muds in the southern North Sea. Mar. Geol. 398, 48–58. https://doi.org/10.1016/J.MARGEO.2017.12.011.

Asmala, E., Carstensen, J., Conley, D.J., Slomp, C.P., Stadmark, J., Voss, M., 2017. Efficiency of the coastal filter: nitrogen and phosphorus removal in the Baltic Sea. Limnol. Oceanogr. 62, S222–S238. https://doi.org/10.1002/lno.10644.

Becherer, J., Flöser, G., Umlauf, L., Burchard, H., 2016. Estuarine circulation versus tidal pumping: sediment transport in a well-mixed tidal inlet. J. Geophys. Res. Ocean. 121, 6251–6270. https://doi.org/10.1002/2016JC011640.

Becker, G.A., Dick, S., Dippner, J.W., 1992. Hydrography of the German bight. Mar. Ecol. Prog. Ser. 91, 9–18.

Blattmann, T.M., Liu, Z., Zhang, Y., Zhao, Y., Haghipour, N., Montluçon, D.B., Plötze, M., Eglinton, T.I., 2019. Mineralogical control on the fate of continentally derived organic matter in the ocean. Science 366, 742–745. https://doi.org/10.1126/science.aax5345.

Brenon, I., Le Hir, P., 1999. Modelling the turbidity maximum in the Seine estuary (France): identification of formation processes. Estuar. Coast. Shelf Sci. 49, 525–544. https://doi.org/10.1006/ECSS.1999.0514.

Du, Z., Yu, Q., Peng, Y., Wang, L., Lin, H., Wang, Y., Gao, S., 2022. The formation of coastal turbidity maximum by tidal pumping in well-mixed inner shelves. J. Geophys. Res. Ocean. 127 https://doi.org/10.1029/2022JC018478.

Dyer, K.R., 1989. Sediment processes in estuaries: future research requirements. J. Geophys. Res. Ocean. 94, 14327–14339. https://doi.org/10.1029/JC094IC10P14327.

Dyer, K.R., Moffat, T.J., 1998. Fluxes of suspended matter in the East Anglian plume, Southern North Sea. Cont. Shelf Res. 18, 1311–1331. https://doi.org/10.1016/S0278-4343(98)00045-4.

Ehrhardt, M., Koeve, W., 1999. Determination of particulate organic carbon and nitrogen. In: Grasshoff, K., Kremling, K., Ehrhardt, M. (Eds.), Methods of Seawater Analysis, 3rd ed. Wiley, pp. 437–444. https://doi.org/10.1002/9783527613984.ch17.

Eisma, D., 1981. Supply and deposition of suspended matter in the North Sea. In: Nio, S.-D., Shüttenhelm, R.T.E., Van Weering, T.C.E. (Eds.), Holocene Marine Sedimentation in the North Sea Basin. Blackwell Publishing Ltd., Oxford, UK, pp. 415–428.

Eisma, D., 1986. Flocculation and de-flocculation of suspended matter in estuaries. Neth. J. Sea Res. 20, 183–199. https://doi.org/10.1016/0077-7579(86)90041-4.

Eisma, D., Kalf, J., 1987. Distribution, organic content and particle size of suspended matter in the North Sea. Neth. J. Sea Res. 21, 265–285. https://doi.org/10.1016/0077-7579(87)90002-0.

Engel, A., Endres, S., Galgani, L., Schartau, M., 2020. Marvelous marine microgels: on the distribution and impact of gel-like particles in the oceanic water-column. Front. Mar. Sci. 7 https://doi.org/10.3389/FMARS.2020.00405/FULL.

Fettweis, M., Baeye, M., 2015. Seasonal variation in concentration, size and settling velocity of muddy marine flocs in the benthic boundary layer. J. Geophys. Res. Oceans 120, 5648–5667. https://doi.org/10.1002/2014JC010644.

Fettweis, M., Houziaux, J.-S., Du Four, I., et al., 2009. Long-term influence of maritime access works on the distribution of cohesive sediments: analysis of historical and recent data from the Belgian nearshore area (southern North Sea). Geo-Marine Lett. 29, 321–330. https://doi.org/10.1007/S00367-009-0161-7/METRICS.

Fettweis, M., Schartau, M., Desmit, X., Lee, B.J., Terseleer, N., Van der Zande, D., Parmentier, K., Riethmüller, R., 2022. Organic matter composition of biomineral flocs and its influence on suspended particulate matter dynamics along a nearshore to offshore transect. J. Geophys. Res. Biogeosciences 127, e2021JG006332. https://doi.org/10.1029/2021JG006332.

Flemming, B.W., Delafontaine, M.T., 2000. Mass physical properties of muddy intertidal sediments: some applications, misapplications and non-applications. Cont. Shelf Res. 20, 1179–1197. https://doi.org/10.1016/S0278-4343(00)00018-2.

Gerritsen, H., Boon, J.G., Van der Kaaij, T., Vos, R.J., 2001. Integrated modelling of suspended matter in the North Sea. Estuar. Coast. Shelf Sci. 53, 581–594. https://doi.org/10.1006/ECSS.2000.0633.

Ho, Q.N., Fettweis, M., Spencer, K.L., Lee, B.J., 2022. Flocculation with heterogeneous composition in water environments: a review. Water Res. 213, 118147 https://doi.org/10.1016/j.watres.2022.118147.

Huthnance, J.M., 1991. Physical oceanography of the North Sea. Ocean Shorel. Manag. 16, 199–231. https://doi.org/10.1016/0951-8312(91)90005-M.

Ittekkot, V., Laane, R.W.P.M., 1991. Fate of riverine particulate organic matter. In: Degens, E.T., Kempe, S., Richey, J.E. (Eds.), Biogeochemistry of Major World Rivers, SCOPE Report 42. Wiley, Chichester, pp. 229–239.

Jago, C.F., Bale, A.J., Green, M.O., et al., 1994. Resuspension processes and seston dynamics, southern North Sea, p. 97–113. In: Charnock, H., Dyer, K.R., Huthnance, J.M., Liss, P.S., Simpson, J.H., Tett, P.B. (Eds.), Understanding the North Sea System. Chapman & Hall, for the Royal Society, Springer, Dordrecht.

Jung, A.S., Bijkerk, R., Van Der Veer, H.W., Philippart, C.J.M., 2017. Spatial and temporal trends in order richness of marine phytoplankton as a tracer for the

exchange zone between coastal and open waters. J. Mar. Biol. Assoc. United Kingdom 97, 477–489. https://doi.org/10.1017/S0025315416001326.
Keil, R.G., Montluçon, D.B., Prahl, F.G., Hedges, J.I., 1994. Sorptive preservation of labile organic matter in marine sediments. Nature 370, 549–552. https://doi.org/10.1038/370549a0.
Kopte, R., Becker, M., Holtermann, P., Winter, C., 2022. Tides, stratification, and counter rotation: the German bight ROFI in comparison to other regions of freshwater influence. J. Geophys. Res. Ocean. 127, e2021JC018236 https://doi.org/10.1029/2021JC018236.
Maerz, J., Hofmeister, R., Van Der Lee, E.M., Gräwe, U., Riethmüller, R., Wirtz, K.W., 2016. Maximum sinking velocities of suspended particulate matter in a coastal transition zone. Biogeosciences 13, 4863–4876. https://doi.org/10.5194/BG-13-4863-2016.
Maggi, F., Tang, F.H.M., 2015. Analysis of the effect of organic matter content on the architecture and sinking of sediment aggregates. Mar. Geol. 363, 102–111. https://doi.org/10.1016/j.margeo.2015.01.017.
Manheim, T.F., Hathaway, J.C., Uchupi, E., 1972. Suspended matter in surface waters of the Northern Gulf of Mexico. Limnol. Oceanogr. 17, 17–27. https://doi.org/10.4319/lo.1972.17.1.0017.
Moulton, M., Suanda, S.H., Garwood, J.C., Kumar, N., Fewings, M.R., Pringle, J.M., 2023. Exchange of plankton, pollutants and particles across the nearshore region. Ann. Rev. Mar. Sci. 15 (1), 167–202. https://doi.org/10.1146/annurev-marine-032122-115057.
Nechad, B., Ruddick, K., Neukermans, G., 2009. Calibration and validation of a generic multisensor algorithm for mapping of turbidity in coastal waters. In: SPIE "Remote Sensing of the Ocean, Sea Ice, and Large Water Regions" Conference held in Berlin (Germany), 31 August 2009. Proc. SPIE Vol. 7473, 74730H.
Nechad, B., Ruddick, K.G., Park, Y., 2010. Calibration and validation of a generic multisensor algorithm for mapping of total suspended matter in turbid waters. Remote Sens. Environ. 114, 854–866.
Neukermans, G., Ruddick, K., Loisel, H., 2012. Optimization and quality control of suspended particulate matter concentration measurement using turbidity measurements. Limnol. Oceanogr. Methods 10, 1011–1023. https://doi.org/10.4319/LOM.2012.10.1011.
Novoa, S., Doxaran, D., Ody, A., et al., 2017. Atmospheric corrections and multi-conditional algorithm for multi-sensor remote sensing of suspended particulate matter in low-to-high turbidity levels coastal waters. Remote Sens. (Basel) 9, 61. https://doi.org/10.3390/RS9010061.
Otto, L., Zimmerman, J.T.F., Furnes, G.K., Mork, M., Saetre, R., Becker, G., 1990. Review of the physical oceanography of the North Sea. Netherlands J. Sea Res. 26, 161–238. https://doi.org/10.1016/0077-7579(90)90091-T.
Pawlowicz, R., 2020. M_Map: A mapping package for MATLAB, version 1.4 m [Computer software], available online at www.eoas.ubc.ca/~rich/map.html.
Pietrzak, J.D., de Boer, G.J., Eleveld, M.A., 2011. Mechanisms controlling the intra-annual mesoscale variability of SST and SPM in the southern North Sea. Cont. Shelf Res. 31, 594–610. https://doi.org/10.1016/j.csr.2010.12.014.
Postma, H., 1981. Exchange of materials between the North Sea and the Wadden Sea. Mar. Geol. 40, 199–213. https://doi.org/10.1016/0025-3227(81)90050-5.
Postma, H., 1984. Introduction to the symposium on organic matter in the Wadden Sea. Netherlands Inst. Sea Res. - Publ. Ser. 10, 15–22.
Prandle, D., Ballard, G., Flatt, D., et al., 1996. Combining modelling and monitoring to determine fluxes of water, dissolved and particulate metals through the Dover Strait. Cont. Shelf Res. 16, 237–257. https://doi.org/10.1016/0278-4343(95)00009-P.
Prandle, D., Hydes, D.J., Jarvis, J., McManus, J., 1997. The seasonal cycles of temperature, salinity, nutrients and suspended sediment in the southern North Sea in 1988 and 1989. Estuar. Coast. Shelf Sci. 45, 669–680. https://doi.org/10.1006/ecss.1996.0227.
Rijnsburger, S., van der Hout, C., van Tongeren, O., de Boer, G., van Prooijen, B.C., Borst, W.G., Pietrzak, J.D., 2016. Simultaneous measurements of tidal straining and advection at two parallel transects far downstream in the Rhine ROFI. Ocean Dyn. 66, 719–736. https://doi.org/10.1007/s10236-016-0947-x.
Röttgers, R., Heymann, K., Krasemann, H., 2014. Suspended matter concentrations in coastal waters: methodological improvements to quantify individual measurement uncertainty. Estuar. Coast. Shelf Sci. 151, 148–155. https://doi.org/10.1016/j.ecss.2014.10.010.
Schartau, M., Riethmüller, R., Flöser, G., van Beusekom, J.E.E., Krasemann, H., Hofmeister, R., Wirtz, K., 2019. On the separation between inorganic and organic fractions of suspended matter in a marine coastal environment. Prog. Oceanogr. 171, 231–250. https://doi.org/10.1016/j.pocean.2018.12.011.
Simpson, J.H., Brown, J., Matthews, J., Allen, G., 1990. Tidal straining, density currents, and stirring in the control of estuarine stratification. Estuaries 13, 125–132. https://doi.org/10.2307/1351581/METRICS.
Stavn, R.H., Rick, H.J., Falster, A.V., 2009. Correcting the errors from variable sea salt retention and water of hydration in loss on ignition analysis: implications for studies of estuarine and coastal waters. Estuar. Coast. Shelf Sci. 81, 575–582. https://doi.org/10.1016/j.ecss.2008.12.017.
Van Leeuwen, S., Tett, P., Mills, D., van der Molen, J., 2015. Stratified and nonstratified areas in the North Sea: long-term variability and biological and policy implications. J. Geoph. Res. Ocean. 120, 4670–4686. https://doi.org/10.1002/2014JC010485.
Yu, M., Yu, X., Mehta, A.J., Manning, A.J., 2023. Persistent reshaping of cohesive sediment towards stable flocs by turbulence. Sci. Rep. 13, 1760. https://doi.org/10.1038/s41598-023-28960-y.